

File ID        uvapub:34321  
Filename      152365y.pdf  
Version        unknown

---

SOURCE (OR PART OF THE FOLLOWING SOURCE):

Type            article  
Title            Discovery of kHz QPO in the Z source cygnus X-1  
Author(s)       R.A.D. Wijnands, J. Homan, M. van der Klis, E. Kuulkers, J.A. van Paradijs,  
                    W.H.G. Lewin, F.K. Lamb, D. Psaltis, B.A. Vaughan  
Faculty         FNWI: Astronomical Institute Anton Pannekoek (IAP)  
Year             1998

FULL BIBLIOGRAPHIC DETAILS:

<http://hdl.handle.net/11245/1.140505>

---

*Copyright*

*It is not permitted to download or to forward/distribute the text or part of it without the consent of the author(s) and/or copyright holder(s), other than for strictly personal, individual use, unless the work is under an open content licence (like Creative Commons).*

---

## DISCOVERY OF kHz QUASI-PERIODIC OSCILLATIONS IN THE Z SOURCE CYGNUS X-2

RUDY WIJNANDS,<sup>1</sup> JEROEN HOMAN,<sup>1</sup> MICHIEL VAN DER KLIS,<sup>1</sup> ERIK KUULKERS,<sup>2</sup> JAN VAN PARADIJS,<sup>1,3</sup> WALTER H. G. LEWIN,<sup>4</sup>  
FREDERICK K. LAMB,<sup>5</sup> DIMITRIOS PSALTIS,<sup>6</sup> AND BRIAN VAUGHAN<sup>7</sup>  
*Received 1997 October 6; accepted 1997 November 18; published 1998 January 14*

### ABSTRACT

During observations with the *Rossi X-Ray Timing Explorer* from 1997 June 31 to July 3 we discovered two simultaneous kHz quasi-periodic oscillations (QPOs) near 500 and 860 Hz in the low-mass X-ray binary and Z source Cygnus X-2. In the X-ray color-color diagram and hardness-intensity diagram (HID), a clear Z track was traced out, which shifted in the HID within 1 day to higher count rates at the end of the observation. Z track shifts are well known to occur in Cyg X-2; our observation for the first time catches the source in the act. A single kHz QPO peak was detected at the left end of the horizontal branch (HB) of the Z track, with a frequency of  $731 \pm 20$  Hz and an amplitude of  $4.7^{+0.8}_{-0.6}\%$  rms in the energy band 5.0–60 keV. Further to the right on the HB, at somewhat higher count rates, an additional peak at  $532 \pm 43$  Hz was detected with an rms amplitude of  $3.0^{+1.0}_{-0.7}\%$ . When the source moved down the HB, thus when the inferred mass accretion rate increased, the frequency of the higher frequency QPO increased to  $839 \pm 13$  Hz, and its amplitude decreased to  $3.5^{+0.4}_{-0.3}\%$  rms. The higher frequency QPO was also detected on the upper normal branch (NB) with an rms amplitude of  $1.8^{+0.6}_{-0.4}\%$  and a frequency of  $1007 \pm 15$  Hz; its peak width did not show a clear correlation with inferred mass accretion rate. The lower frequency QPO was most of the time undetectable, with typical upper limits of 2% rms; no conclusion on how this QPO behaved with mass accretion rate can be drawn. If the peak separation between the QPOs is the neutron star spin frequency (as required in some beat-frequency models), then the neutron star spin period is  $2.9 \pm 0.2$  ms ( $346 \pm 29$  Hz). This discovery makes Cyg X-2 the fourth Z source that displays kHz QPOs. The properties of the kHz QPOs in Cyg X-2 are similar to those of other Z sources.

Simultaneous with the kHz QPOs, the well-known horizontal-branch QPOs (HBOs) were visible in the power spectra. At the left end of the HB, the second harmonic of the HBO was also detected. We also detected six small X-ray bursts. No periodic oscillations or QPOs were detected in any of them, with typical upper limits of 6%–8% rms.

*Subject headings:* accretion, accretion disks — stars: individual (Cygnus X-2) — stars: neutron — X-rays: stars

### 1. INTRODUCTION

The low-mass X-ray binary (LMXB) and Z source (Hasinger & van der Klis 1989) Cyg X-2 is one of the best studied LMXBs. In the X-ray color-color diagram (CD), a Z-shaped track is traced out. Its branches are called horizontal branch (HB), normal branch (NB), and flaring branch (FB). The rapid X-ray variability in Z sources is closely related to the position of the sources on the Z. Quasi-periodic oscillations (QPOs) are present on the HB and the upper NB with a frequency between 18 and 60 Hz (called HBO). QPOs with a frequency between 5 and 20 Hz are present on the lower part of the NB and on the beginning of the FB (called N/FBOs). Both the X-ray spec-

tral changes and the rapid X-ray variability are thought to be due to changes in the mass accretion rate ( $\dot{M}$ ) (see, e.g., Hasinger & van der Klis 1989; Lamb 1991), which is inferred to be lowest on the HB, increasing along the Z and reaching the Eddington mass accretion rate at the NB/FB vertex.

Recent studies of Cyg X-2 (*EXOSAT*, Kuulkers, van der Klis, & Vaughan 1996; *Ginga*, Wijnands et al. 1997a) show that Cyg X-2 displays motion of the Z track in the hardness-intensity diagram (HID). Following Kuulkers et al. (1996), we call the different positions of the Z track in the HID different “overall intensity levels.” When the overall intensity level changes, the morphology of the Z changes and the whole Z moves in the CD as well as in the HID. Wijnands et al. (1997a) found that the X-ray timing behavior on the lower part of the NB differs significantly for different overall intensity levels. The fact that the X-ray spectral and X-ray timing behavior change with changing overall intensity level suggests that something else in addition to  $\dot{M}$  determines the Z track and the timing properties of Cyg X-2. A precessing accretion disk, strongly suggested by the 78 day period found in Cyg X-2 using the *ASM/RXTE* long-term X-ray light curve (Wijnands, Kuulkers, & Smale 1996), is a possible explanation of the long-term changes.

In numerous LMXBs, mostly atoll sources (Hasinger & van der Klis 1989), kHz QPOs have been observed (see van der Klis 1998 for a recent review on kHz QPO properties). So far, kHz QPOs have been found in three Z sources (Sco X-1, van der Klis et al. 1996a, 1997; GX 5–1, van der Klis et al. 1996b;

<sup>1</sup> Astronomical Institute “Anton Pannekoek,” University of Amsterdam, and Center for High Energy Astrophysics, Kruislaan 403, NL-1098 SJ, Amsterdam, The Netherlands; rudy@astro.uva.nl, homan@astro.uva.nl, michiel@astro.uva.nl, jvp@astro.uva.nl.

<sup>2</sup> Astrophysics, University of Oxford, Nuclear and Astrophysics Laboratory, Keble Road, Oxford OX1 3RH, England, UK; e.kuulkers1@physics.oxford.ac.uk.

<sup>3</sup> Departments of Physics, University of Alabama at Huntsville, Huntsville, AL 35899.

<sup>4</sup> Department of Physics and Center for Space Research, Massachusetts Institute of Technology, Cambridge, MA 02139; lewin@space.mit.edu.

<sup>5</sup> Departments of Physics and Astronomy, University of Illinois at Urbana-Champaign, Urbana, IL 61801; f-lamb@uiuc.edu.

<sup>6</sup> Harvard-Smithsonian Center for Astrophysics, 60 Garden Street, Cambridge, MA 02138; demetris@cfata1.harvard.edu.

<sup>7</sup> Space Radiation Laboratory, California Institute of Technology, 220-47 Downs, Pasadena, CA 91125; brian@thor.srl.caltech.edu.

GX 17+2, Wijnands et al. 1997b). In this Letter, we report the discovery of two simultaneous kHz QPOs in the Z source Cyg X-2.

## 2. OBSERVATIONS AND ANALYSIS

We observed Cyg X-2 with the *Rossi X-Ray Timing Explorer* (*RXTE*) from 1997 June 30 until July 3. A total of 108 ks of data was obtained. Data were collected simultaneously with 16 s time resolution in 129 photon energy channels (effective energy range 2–60 keV), and with 122  $\mu$ s time resolution in two channels (2–5.0 keV, 5.0–60 keV). A CD and HID were made using the 16 s data, and power density spectra were calculated from the 122  $\mu$ s data using 16 s data segments.

For measuring the kHz QPO properties, we fitted the 128–4096 Hz power spectra with a constant plus a broad sinusoid representing the dead-time–modified Poisson level (Zhang 1995; Zhang et al. 1995), and one or two Lorentzian peaks representing the kHz QPOs. For measuring the HBO, we fitted the 8–256 Hz power spectra with a constant plus a power law representing the continuum, and one or two Lorentzian peaks representing the HBO and its second harmonic. Differential dead-time effects (van der Klis 1989) were negligible due to the relatively low count rates. The errors on the fitted parameters were determined using  $\Delta\chi^2 = 1.0$ ; upper limits were determined using  $\Delta\chi^2 = 2.71$ , corresponding to 95% confidence levels. The kHz QPOs were only detected in the 5.0–60 keV band. In the 2–5.0 keV and the combined 2–60 keV energy bands, the kHz QPOs were undetectable. Therefore, we used the 5.0–60 keV band throughout our analysis.

For the CD we used for the soft color the logarithm of the count rate ratio between 3.5–6.4 keV and 2.0–3.5 keV, and for the hard color we used the logarithm of the ratio between 9.7–16.0 keV and 6.4–9.7 keV. For the HID we used as intensity the logarithm of the count rates in the energy band 2.0–16.0 keV, and for the hardness we used the hard color from the CD. For  $\sim 12\%$  of the time, detector 4 or 5 was off. For the CD and HID we only used the data of the three detectors, which were always on in order to get the position of Cyg X-2 on the Z during the whole observation. For the power density spectra, we used all available data.

We used the  $S_z$  parameterization (see Wijnands et al. 1997a and references therein) for measuring the position along the Z (HB/NB vertex at  $S_z = 1$ , NB/FB vertex at  $S_z = 2$ ). Owing to the fact that the position on the Z could be much better determined in the HID than in the CD, we used the  $S_z$  parameterization for the Z track in the HID. Thus, the  $S_z$ -values quoted in this Letter represent the position of the source on the Z track in the HID. By using logarithmic values for the colors and the intensity,  $S_z$  does not depend on the values of those quantities but only on their variations (Wijnands et al. 1997a).

## 3. RESULTS

In Figure 1, the CD and the HID are shown. Cyg X-2 traced out an almost complete Z track. The HID (Fig. 1b) clearly shows that part of the data near the HB/NB vertex (regions 8, 9, and 11 in Fig. 1b) was shifted to a higher count rate with respect to the rest. No sudden jump in count rate is visible in the X-ray light curve so Cyg X-2 moved smoothly to higher count rates. At the end of the observation, the source moved in 0.7 days from the HB/NB vertex to the left of the HB and back to the vertex again, which by then had shifted to higher count rates. This is the first time we catch the source in the act. Previously, shifted Z's were only detected on timescales

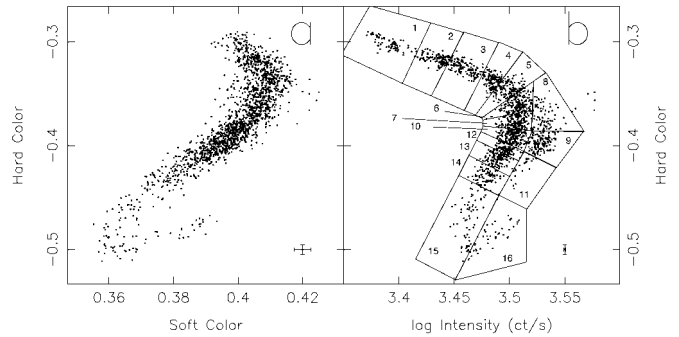


FIG. 1.—Color-color diagram (a) and hardness-intensity diagram (b) of Cyg X-2. The soft color is the logarithm of the count rate ratio between 3.5–6.4 keV and 2.0–3.5 keV; the hard color is the logarithm of the count rate ratio between 9.7–16.0 keV and 6.4–9.7 keV; the intensity is the logarithm of the 3-detector count rate in the photon energy range 2.0–16.0 keV. Both diagrams are corrected for background ( $\sim 50$  counts  $s^{-1}$  in the energy range 2.0–16.0 keV); the count rate is not dead-time corrected (4%–6% correction). All points are 64 s averages. Typical error bars are shown at the bottom right corners of the diagrams. The boxes in the HID are the regions that were selected to study the timing behavior.

of weeks to months (between observations), not during one observation. In the CD (Fig. 1a) the shift is not visible due to the fact that this shift takes place parallel to the NB (see also Wijnands et al. 1997a), and therefore all data overlap. Also, the error bars in the CD are large, giving larger uncertainties than in the HID. Some of the timing properties have previously been observed to change when the Z track shifts in the CD and HID (Wijnands et al. 1997a). For the small shift in the Z track in our observation, these changes were undetectable for the QPOs discussed in this Letter.

Between 1997 July 2 UT 03:36 and 08:19 (5.8 ks exposure time) we detected two simultaneous kHz QPOs (Fig. 2a) with frequencies of  $516 \pm 27$  and  $862 \pm 11$  Hz (peak separation of  $346 \pm 29$  Hz), at  $3.4 \sigma$  and  $4.4 \sigma$  significance, respectively. The FWHM and rms amplitude were  $170^{+66}_{-51}$  Hz and  $3.6^{+0.6}_{-0.5}\%$  for the lower frequency QPO, and  $94^{+31}_{-25}$  Hz and  $3.5\% \pm 0.4\%$  for the higher frequency QPO. Upper limits to the rms amplitude of the QPOs for the same time interval in the energy range 2–5.0 keV were 2.4% and 1.1% rms, respectively. Simultaneously with these kHz QPO we detected the HBO. Between 1997 July 2 UT 09:37 and 12:57 (7 ks exposure time), we detected a single kHz QPO (Fig. 2b) with a frequency of  $779 \pm 16$  Hz at  $4.9 \sigma$  significance, with a FWHM of  $177^{+52}_{-40}$  Hz, and an amplitude of  $4.7^{+0.6}_{-0.5}\%$  rms. The upper limit on the amplitude of the QPO in the 2–5.0 keV band was 2.7% rms; kHz QPOs were detected at several other times, although usually below a  $3 \sigma$  significance level.

The Z track in the HID was not homogeneously covered. In order to get enough statistics to detect the kHz QPOs or determine useful upper limits at all positions on the Z track, we selected power spectra in the regions of the HID indicated in Figure 1b. Afterward, we determined the average  $S_z$ -value of the power spectra selected. The frequency and the rms amplitudes of the kHz QPOs versus  $S_z$  are shown in Figure 3. At the leftmost end of the HB (lowest count rates), only the higher frequency QPO could be detected. When the source moved to somewhat higher count rates, a second, lower frequency kHz QPO became detectable. Further to the right on the HB, the lower frequency kHz QPO was undetectable again with upper limits of 2%–3%. Near the HB/NB vertex, the higher frequency QPO was detected, but further down the NB the higher fre-

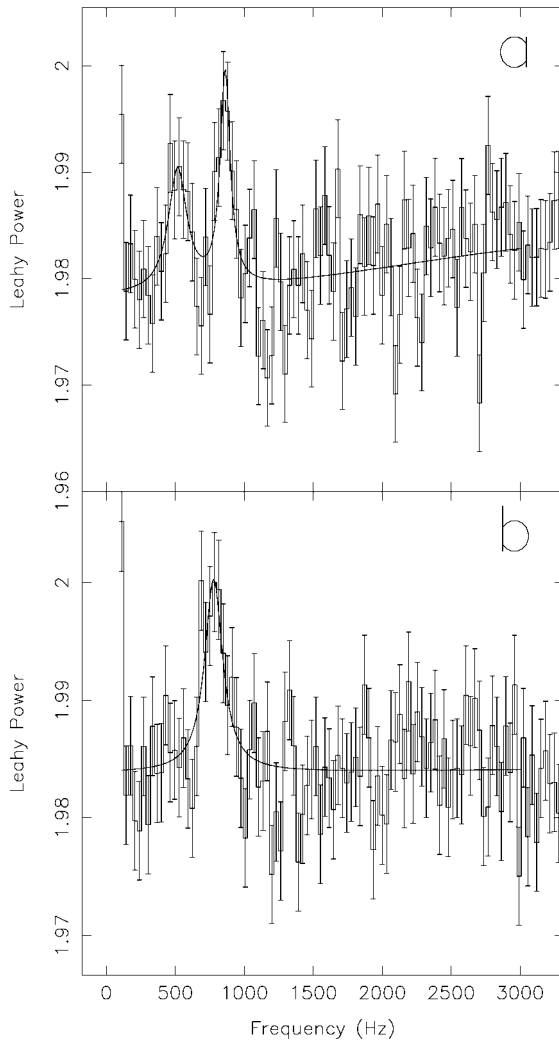


FIG. 2.—Typical Leahy normalized power spectra in the energy range 5.0–60 keV showing the kHz QPOs. The upward slope at kHz frequencies is due to instrumental dead time. (a) Power spectrum for the interval 1997 July 2 UT 03:36–08:19; (b) power spectrum for the interval 1997 July 2 UT 09:37–12:57.

quency peak became undetectable, with upper limits of 2%–4% rms. With increasing  $\dot{M}$ , the frequencies of the higher frequency kHz QPOs increased and its amplitude decreased (Figs. 3a and 3c). The FWHM of the peak did not show a clear correlation with  $\dot{M}$ . Owing to the small number of detections of the lower frequency QPO, no conclusions can be drawn about the behavior of this QPO with  $\dot{M}$ , although there are indications that its frequency also increases with  $\dot{M}$  (see Fig. 3a). It was not possible to determine if the kHz QPO properties changed significantly as the Z track moved in the HID (regions 6, 7, and 12 vs. 8 and 9 in Fig. 1b). This was also true for the properties of the HBO.

Simultaneously with the kHz QPOs, we detected the HBO. Its properties (in the 5.0–60 keV band) versus  $S_z$  are also shown in Figure 3. The HBO second harmonic was only detectable in region 1 ( $S_z = -0.09 \pm 0.1$ ) of Figure 1b with a frequency of  $73.6 \pm 0.8$  Hz, an rms amplitude of  $3.1^{+0.2}_{-0.4}$ %, and a FWHM of  $13^{+2}_{-3}$  Hz. The HBO fundamental in this region had a frequency of  $36.2 \pm 0.2$  Hz, an rms amplitude of  $4.5^{+0.1}_{-0.3}$ %, and a FWHM of  $6.8^{+0.4}_{-0.7}$  Hz. When the source moved further to the right on the HB, the second harmonic became undetectable

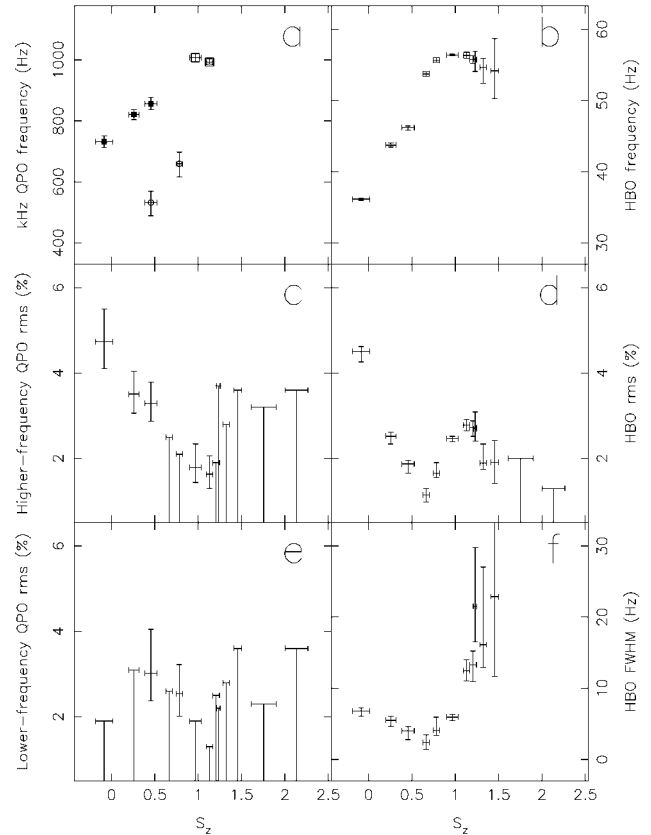


FIG. 3.—(a) Frequency of the kHz QPOs; (b) frequency of the HBO fundamental; (c) the rms amplitude of the higher frequency kHz QPO; (d) the rms amplitude of the HBO fundamental; (e) the rms amplitude of the lower frequency kHz QPO; and (f) the FWHM of the HBO fundamental as a function of  $S_z$ . In (a) the squares represent the higher frequency QPO and the circles the lower frequency QPOs. Open symbols represent detections of the kHz QPOs with significance between a  $2\sigma$  and  $3\sigma$ ; the filled points represent detections with greater than  $3\sigma$  significance.

with typical upper limits on the amplitude of 1%–2% rms. The HBO fundamental was detected to about halfway down the NB (region 14;  $S_z = 1.46 \pm 0.05$ ). Its frequency increases from  $36.2 \pm 0.2$  Hz at the left end of the HB to  $56.4 \pm 0.1$  Hz at the HB/NB vertex (Fig. 3b). After that its frequency remained approximately constant. The rms amplitude of the HBO first decreased on the HB with increasing  $\dot{M}$ , but around  $S_z = 0.6$  it started to increase again (Fig. 3d). At around  $S_z = 1.1$  it decreased again with increasing  $\dot{M}$  until it became undetectable further down the NB. Its FWHM also first decreased on the HB with increasing  $\dot{M}$  (Fig. 3f), and at the same position on the Z where the amplitude of the HBO started to increase again with increasing  $\dot{M}$ , the FWHM also started to increase again.

We detected six bursts in the X-ray light curve (typical durations of 4–6 s) that are very similar to those found in *EXOSAT* (Kuulkers, van der Klis, & van Paradijs 1995) and *Ginga* (Wijnands et al. 1997a) data. We searched for periodic oscillations and QPOs during the bursts, but none were detected (typical upper limits of 6%–8% rms). A more detailed study of the X-ray bursts will be reported elsewhere.

#### 4. DISCUSSION

We have discovered two simultaneous kHz QPOs near 500 and 860 Hz in the Z source Cyg X-2. The frequency of the

higher frequency QPO increased when the source moved from the left end of the HB to the upper NB, and there are indications that the same is true for the frequency of the lower frequency QPO. Cyg X-2 is the fourth Z source that displays kHz QPOs. Most likely the remaining two Z sources (GX 340+0 and GX 349+2) will also display kHz QPOs when they are observed on the (left end of the) HB (note that GX 349+2 has never been observed in the HB).

The properties of the kHz QPOs in Z sources are very similar to each other. In each source the kHz QPOs increase in frequency and the higher frequency QPO decreases in amplitude when the sources move down the Z, thus when  $\dot{M}$  increases. The amplitude of the lower frequency QPO and the FWHM of the peaks do not have a clear correlation with  $\dot{M}$ . The kHz QPOs in Z sources are also very similar to what is observed (see, e.g., Strohmayer et al. 1996; Zhang et al. 1996; Berger et al. 1996; Smale et al. 1997) in other, less luminous LMXBs (the atoll sources; Hasinger & van der Klis 1989). In both types of sources, the frequency of the kHz QPOs increases with inferred  $\dot{M}$ , the kHz QPOs are strongest in the highest photon energy band, the maximum frequencies so far detected are between 1000 and 1200 Hz, and the separation between the kHz QPOs lies between 250 and 370 Hz (see van der Klis 1998 for a recent review on kHz QPO properties). Therefore, it seems likely that kHz QPOs in atoll sources and in Z sources are produced by the same mechanism.

In Sco X-1 (van der Klis et al. 1996a, 1997) the peak separation between the two kHz QPOs decreases with increasing  $\dot{M}$ .<sup>8</sup> In GX 17+2 a similar decrease in peak separation could not be excluded (Wijnands et al. 1997b), and owing to the sparsity of detections with two simultaneous kHz QPO in the present data, nothing can be said for Cyg X-2. If the peak separation was a measure for the neutron spin frequency, then the spin frequency in Cyg X-2 is  $346 \pm 29$  Hz (spin period of  $2.9 \pm 0.2$  ms). In the four Z sources for which kHz QPOs have been discovered, the kHz QPOs were detected simultaneously with the HBO, ruling out the possibility that both the HBOs

<sup>8</sup> Recently, Méndez et al. (1998) found that also in the atoll source 4U 1608–52 the peak separation may not be constant.

and the kHz QPOs are magnetospheric beat frequencies (van der Klis et al. 1997).

At the left end of the HB, the amplitude, in the energy range 5–60 keV, of the higher frequency QPO in Cyg X-2 is  $4.7_{-0.6}^{+0.8}\%$  rms. This amplitude is smaller than the typical amplitudes of the kHz QPOs in the atoll sources, which are thought to have significantly weaker magnetic fields, as predicted by the sonic-point model (Miller, Lamb, & Psaltis 1998). The QPOs in Cyg X-2 are similar in strength to those in GX 17+2 (2%–5% rms in 5–60 keV), even though GX 17+2 may have a weaker magnetic field, as suggested by its weaker HBO and by X-ray spectral modeling (Psaltis, Lamb, & Miller 1995). This indicates that if the strength of the stellar magnetic field affects the amplitudes of the kHz QPOs, it is not the only variable that does so, and that other variables, such as the multipolar structure and orientation of the magnetic field, and the spin rate of the star, also play a role. If the orientation of the magnetic field with respect to the plane of the disk plays a role, its effect should be visible in the amplitude of the kHz QPOs in Cyg X-2 when these QPOs are detected during different overall intensity levels, thus at different phases of the 78 day long-term X-ray cycle.

*Note added in manuscript.*—After submission of this Letter we discovered also two simultaneous kHz QPOs in the Z source GX 340+0 at  $348_{-16}^{+20}$  and  $722 \pm 13$  Hz (peak separation of  $374 \pm 24$  Hz, when the source was on the horizontal branch (Jonker et al. 1998). The FWHM and rms amplitude (in the energy range 5.0–60 keV) were  $114_{-39}^{+64}$  Hz and  $2.5_{-0.4}^{+0.5}\%$  for the lower frequency QPO, and  $177_{-45}^{+58}$  Hz and  $3.8_{-0.4}^{+0.5}\%$  for the higher frequency QPO.

This work was supported in part by the Netherlands Foundation for Research in Astronomy (ASTRON) grant 781-76-017 and by NSF grant AST 96-18524. B. V. (NAG 5-3340), F. K. L. (NAG 5-2925), J. v. P. (NAG 5-3269, NAG 5-3271), and W. H. G. L. acknowledge support from the United States National Aeronautics and Space Administration. We thank the *RXTE* Science Operations Facility, and especially John Cannizzo, for rapidly providing the real-time data used in this analysis.

#### REFERENCES

- Berger, M., et al. 1996, *ApJ*, 469, L13  
 Hasinger, G., & van der Klis, M. 1989, *A&A*, 225, 79  
 Kuulkers, E., van der Klis, M., & van Paradijs, J. 1995, *ApJ*, 450, 748  
 Kuulkers, E., van der Klis, M., & Vaughan, B. A. 1996, *A&A*, 311, 197  
 Jonker, P., et al. 1998, in preparation  
 Lamb, F. K. 1991, in *NATO ASI Series C 344, Neutron Stars: Theory and Observations*, ed. J. Ventura & D. Pines (Dordrecht: Kluwer), 445  
 Méndez, M., et al. 1998, *ApJ*, in press  
 Miller, C., Lamb, F. K., & Psaltis, D. 1998, *ApJ*, submitted  
 Psaltis, D., Lamb, F. K., & Miller, G. 1995, *ApJ*, 454, L137  
 Smale, A., Zhang, W., & White, N. E. 1997, *ApJ*, 483, L119  
 Strohmayer, T. E., Zhang, W., Swank, J. H., Smale, A., Titarchuk, L., & Day, C. 1996, *ApJ*, 469, L9  
 van der Klis, M. 1989, in *NATO ASI C262, Timing Neutron Stars*, ed. H. Ögelman & E. P. J. van den Heuvel (Dordrecht: Kluwer), 27  
 van der Klis, M. 1998, in *Proc. NATO Advanced Study Institute, The Many Faces of Neutron Stars*, in press (astro-ph/9710016)  
 van der Klis, M., Swank, J. H., Zhang, W., Jahoda, K., Morgan, E. H., Lewin, W. H. G., Vaughan, B., & van Paradijs, J. 1996a, *ApJ*, 469, L1  
 van der Klis, M., et al. 1996b, *IAU Circ.* 6511  
 van der Klis, M., Wijnands, R. A. D., Horne, K., & Chen, W. 1997, *ApJ*, 481, L97  
 Wijnands, R. A. D., Kuulkers, E., & Smale, A. P. 1996, *ApJ*, 473, L45  
 Wijnands, R. A. D., van der Klis, M., Kuulkers, E., Asai, K., & Hasinger, G. 1997a, *A&A*, 323, 399  
 Wijnands, R., et al. 1997b, *ApJ*, 490, L157  
 Zhang, W. 1995, *XTE/PCA Internal Memo*  
 Zhang, W., Jahoda, K., Swank, J. H., Morgan, E. H., & Giles, A. B. 1995, *ApJ*, 449, 930  
 Zhang, W., Lapidus, I., White, N. E., & Titarchuk, L. 1996, *ApJ*, 469, L17